Ajayi Crowther Journal of Pure and Applied Sciences (ACJPAS)
https://acjpas.acu.edu.ng

Ajayi Crowther J. Pure Appl. Sci. 2023, 2(1), pp. 47-59
https://doi.org/10.56534/acjpas.2023.02.01.47

*Article*

# Seafloor Sediments Morphodynamics: Implications on Subsea Facilities in Mfotu field offshore Eastern Niger Delta Nigeria

**Hope Chibuzor Chuku, Ekaete Enamekere Umoh, Peace Oluwaseyi Agbaje**

Department of Earth Sciences, Faculty of Natural Sciences, Ajayi Crowther University, Oyo, Nigeria.
hc.chuku@acu.edu.ng (H.C.C); ee.umoh@acu.edu.ng (E.E.U); po.agbaje@acu.edu.ng (P.O.A.)

* Correspondence: (H.C.C.) hc.chuku@acu.edu.ng

**Article history:** *Received, Aug. 15, 2022; Revised, Sept. 10, 2022; Accepted, Sept. 15, 2022; Published, Mar. 29, 2023.*

## Abstract

Over 20km cruise of high-frequency 3.5 kHz, echo-sounder, side scan sonar and sub bottom profiler data were collected between October 9th and November 4th 2018 from Mfotu field Eastern Niger Delta with the aim to study the seafloor morphology. The field was divided into two acoustic facies: (a) Type A seabed is of high reflective sediments (sand) found on mid- to outer-section on seafloor less than 15m deep; (b) Type B seabed is of low reflective sediments (silt and clay) between 20 and 25m depth. The prominent seismo-stratigraphic layer was found 45m below the seabed which is the competent bed (lithified sediments) for subsea facilities installations. The acoustic facies were explained in terms of oceanographic influences on the field, there were no impediments to sea-going vessels/rigs navigation and the emplacement of subsea facilities like pipelines, jackets, platforms and cables observed in the study location.

**Keywords:** Sediments, Seabed, Onboard instrumentation, Morphology

## 1. Introduction

Routine application of multibeam sonar bathymetry and backscatter has revolutionized our understanding of continental shelf morphodynamics. The ability to view a near-continuous topographic surface together with variations in seabed backscatter strength provides an overview analogous to aerial photography, resulting in a vastly improved ability to interpret the seafloor sedimentary processes [9]. One of the most immediate results of this new technology has been the recognition, for the first time, of the continuity and juxtaposition of long wavelength features such as drowned beach ridges and reefs [7], or moraine complexes. But the real challenge to maximizing the usefulness of these data lie in the finer details revealed. The detail is in the shorter wavelength morphology that lies close to the limits of resolution of these systems. After the first pass interpretation of the current state of the shelf, future research will be increasingly focused on monitoring their temporal evolution. The first view provides a snapshot. That snapshot allows inferences to be made about likely sedimentary processes. However, proof of the activity of those processes awaits repetitive surveying. Proof that the seabed has changed requires confidence in the absolute accuracy of both the bathymetric and backscatter output of the integrated sonar system. Obvious change, such as new slide scars [2], overprinted iceberg scours [13], freshly emplaced debris flows [12] or significantly migrated bedform positions [6] can be discerned from imperfect data. However, subtler transitions, such as accretion of thin sand sheets, deflation of near shore sand bodies, deepening of pockmarks or migration of ripples requires a level of absolute accuracy that lie at the limit of many of the integrated systems. This paper explores the resolution and accuracy capabilities in both bathymetry and backscatter that is realistically available from currently state of-

the-art multibeam sonar systems. Practical examples are provided, illustrating the advantages and limitations of this sort of data for shelf morphodynamics research.

### 1.1 Study Area and Location

Over the years, many research projects have been conducted within the Niger Delta (Figure 1) making it an increasingly well-documented study locale (Table 1). Though the studies have ranged from sedimentology and stratigraphy, many have looked at the physical and geologic properties of the Basin.

Table 1: Study Area line defining coordinates (Projection: Nigeria West Belt C.M. 004°30' East)

| S/N | Easting (m) | Northing (m) |
|---|---|---|
| **1.** | 295436 | 171836 |
| **2.** | 294567 | 169350 |
| **3.** | 273866 | 196831 |
| **4.** | 274777 | 194365 |
| **5.** | 280746 | 164977 |
| **6.** | 295638 | 173024 |

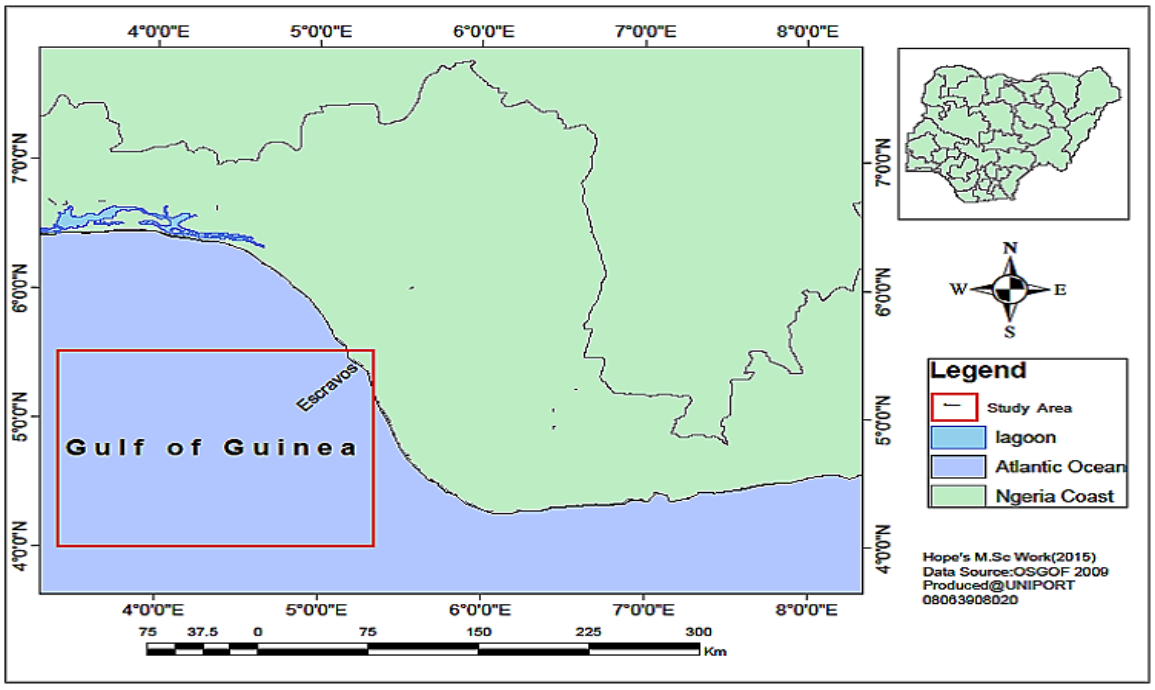


**Figure 1:** Map of the Study Location and coordinates, 25.82km offshore Western Niger Delta Nigeria *(Modified after [4] and [5]).*

## 2. Methods

### *2.1 Calibration*

The Echosounder was function tested at the dock prior to survey. The tests indicated that the transducer was functional. Offshore, the echo sounder was calibrated for bar check and index error. Velocity of sound in water was read and the value obtained was inputed into the echo sounder unit. Further calibration was done by bar check. The index error was found to be less than 0.1m. To clear the error, the draft setting on the echo sounder was adjusted to bring the reading at par with that measured in the bar check[11]. The echo sounder was also checked to have unhindered

communication with the navigation system. The Multibeam system was used to carry out the survey. The equipment was calibrated for patch test: Roll, Heave, Pitch, Yaw and GPS Latency [10]. The multibeam was side mounted and the transducer was defined as the vessel datum in the navigation software. Data acquisition was carried out simultaneously with the analogue survey.All bathymetric data were reduced to metres and decimeters and referenced to the Lowest Astronomical Tide (LAT) using predicted tides Opobo River Approach. The DGPS Receiver was used to carry out the survey. GPS verification was done at the BL jetty in the absence of known survey controls to determine the accuracy of the Receiver. The GPS verification determined the difference between calculated and measured difference between two GPS antennas [1]. The two C-Nav GPS antenna positions were logged simultaneously and the difference was computed in an excel sheet and compared with the measured difference. The difference between the computed and measured distance was 0.3m (Figure 2).

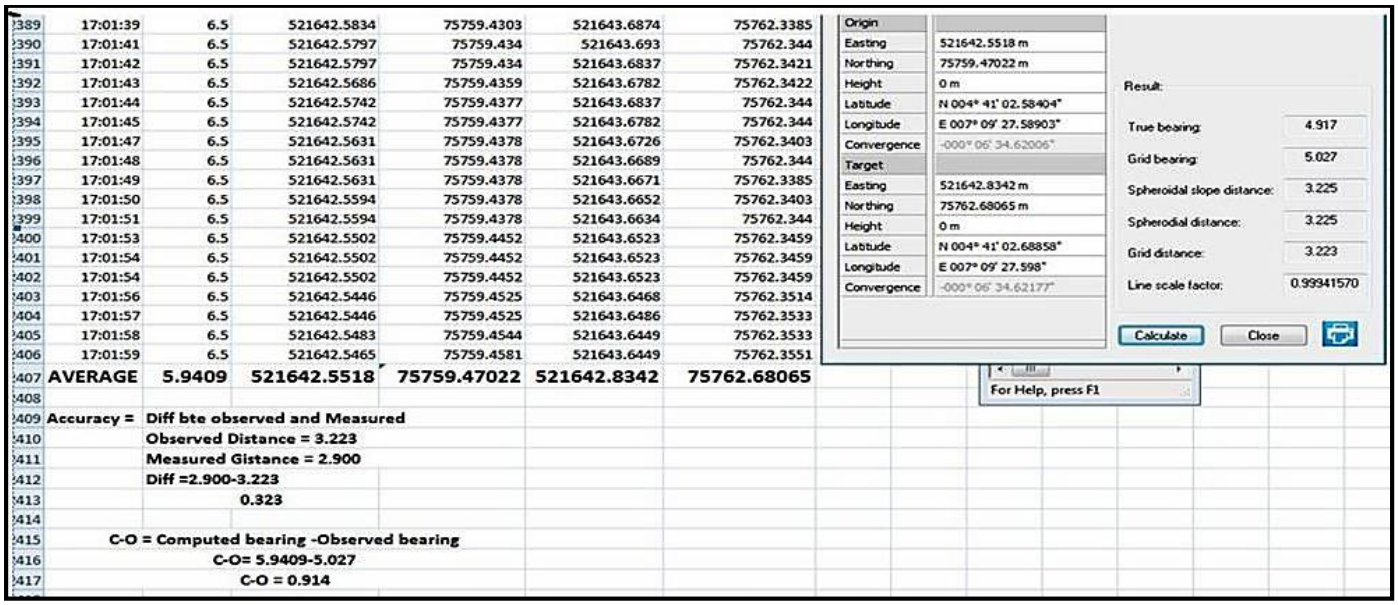

| | | | | | | |
|---|---|---|---|---|---|---|
| 389 | 17:01:39 | 6.5 | 521642.5834 | 75759.4303 | 521643.6874 | 75762.3385 |
| 390 | 17:01:41 | 6.5 | 521642.5797 | 75759.434 | 521643.693 | 75762.344 |
| 391 | 17:01:42 | 6.5 | 521642.5797 | 75759.434 | 521643.6837 | 75762.3421 |
| 392 | 17:01:43 | 6.5 | 521642.5686 | 75759.4359 | 521643.6782 | 75762.3422 |
| 393 | 17:01:44 | 6.5 | 521642.5742 | 75759.4377 | 521643.6837 | 75762.344 |
| 394 | 17:01:45 | 6.5 | 521642.5742 | 75759.4377 | 521643.6782 | 75762.344 |
| 395 | 17:01:47 | 6.5 | 521642.5631 | 75759.4378 | 521643.6726 | 75762.3403 |
| 396 | 17:01:48 | 6.5 | 521642.5631 | 75759.4378 | 521643.6689 | 75762.344 |
| 397 | 17:01:49 | 6.5 | 521642.5631 | 75759.4378 | 521643.6671 | 75762.3385 |
| 398 | 17:01:50 | 6.5 | 521642.5594 | 75759.4378 | 521643.6652 | 75762.3403 |
| 399 | 17:01:51 | 6.5 | 521642.5594 | 75759.4378 | 521643.6634 | 75762.344 |
| 400 | 17:01:53 | 6.5 | 521642.5502 | 75759.4452 | 521643.6523 | 75762.3459 |
| 401 | 17:01:54 | 6.5 | 521642.5502 | 75759.4452 | 521643.6523 | 75762.3459 |
| 402 | 17:01:54 | 6.5 | 521642.5502 | 75759.4452 | 521643.6523 | 75762.3459 |
| 403 | 17:01:56 | 6.5 | 521642.5446 | 75759.4525 | 521643.6468 | 75762.3514 |
| 404 | 17:01:57 | 6.5 | 521642.5446 | 75759.4525 | 521643.6486 | 75762.3533 |
| 405 | 17:01:58 | 6.5 | 521642.5483 | 75759.4544 | 521643.6449 | 75762.3533 |
| 406 | 17:01:59 | 6.5 | 521642.5465 | 75759.4581 | 521643.6449 | 75762.3551 |
| 407 | **AVERAGE** | **5.9409** | **521642.5518** | **75759.47022** | **521642.8342** | **75762.68065** |
| 408 | | | | | | |
| 409 | **Accuracy =** | **Diff bte observed and Measured** | | | | |
| 410 | | **Observed Distance = 3.223** | | | | |
| 411 | | **Measured Gistance = 2.900** | | | | |
| 412 | | **Diff =2.900-3.223** | | | | |
| 413 | | **0.323** | | | | |
| 414 | | | | | | |
| 415 | | **C-O = Computed bearing -Observed bearing** | | | | |
| 416 | | **C-O= 5.9409-5.027** | | | | |
| 417 | | **C-O = 0.914** | | | | |



**Figure 2:** DGPS verification dump sheet.

Positioning was by DGPS. The relative offsets from the GPS antenna to the various survey sensor deployment points were determined using tape measurements. These measurements were independently checked by a different crew member and compared with scale drawings of the vessel. All offsets between the datum point and the antenna / sensors on the survey vessel were taken. The positioning system performed as designed. There was no failure from the C- NAV or crashes from the navigation software.

The Side Scan Sonar equipment was calibrated for Rub test and Range test in water only. The sub-bottom profiler was tested for pinging on the ground and wet test in water. An integrity and function test of the gyro- compass was carried out at the dock prior to mobilization. The gyro- compass was aligned in the direction of the bow of the vessel in the survey room. The captain was directed to turn the vessel in the opposite direction to achieve 180 turn. The gyro- compass readings were within tolerance limits and compared favorably with the vessel's gyro compass.

### *2.2 Data Acquisition*

The survey lines (Figure 3) were designed based on the observations made on sonar records during data acquisition. The specific acoustic equipments such as Side Scan Sonar, Sub-bottom Profiler, Magnetometer and Echo Sounder were deployed during survey to achieve the survey objective. The differential Global Positioning System (DGPS receiver) which tracks up to twenty one satellites at a time, was interfaced with EIVA Navipac navigation and data logging software package to provide reliable, precision (+/- 0.3meter) horizontal positioning. The system outputs position fixes at specified intervals to an onboard accurately. The vessel navigates along preselected survey track lines

throughout the area investigated and data-logging computer which allowed the survey vessel helmsman was used.

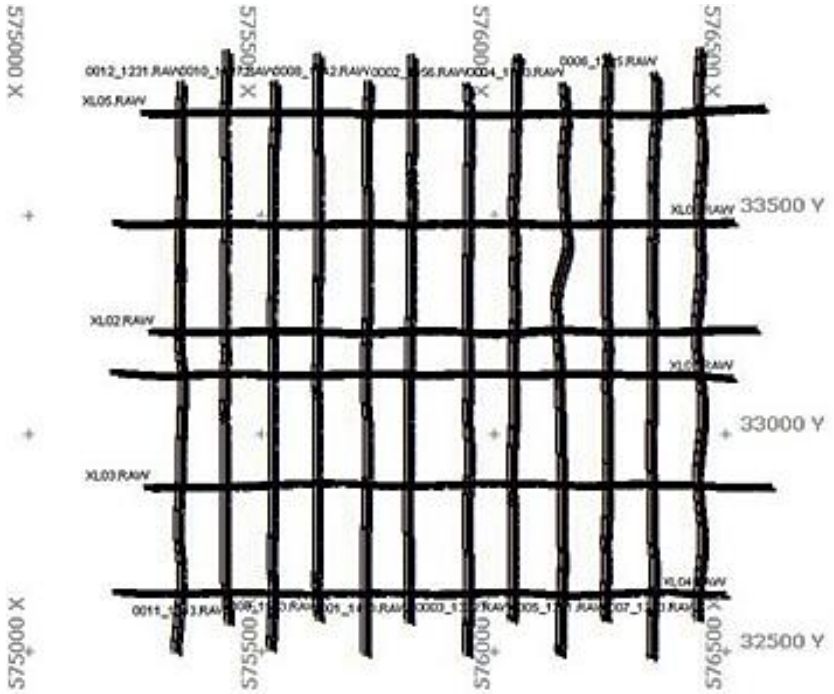


**Figure 3:** Navigation Track plot

### *2.3 Data Processing and Analysis*

#### *2.3.1 Bathymetric Sounding Data*

Digitally recorded depth data were compared with sounding print records produced during the survey for verification of depth quality. Recorded depth data were adjusted for transducer draft (distance between transducer and water surface) and changes in water mass sound speed. The depth data were then referenced to Lowest Astronomical Tide (LAT) in metres by correcting for tidal levels using tidal prediction tables for Opobo River approach (a standard port). The height of water, referenced to LAT, was subtracted from the depth measurement to refer it to datum.

#### *2.3.2 Side Scan Sonar Imagery*

The side scan sonar imagery logged digitally in the field were processed to produce files and plotted in plain view. This plot was then used to characterize the seabed. Seabed characterization was accomplished by interpreting the side-scan sonar records in conjunction with sounding data; sub-bottom data and visual observations.

#### *2.3.3 Subbottom Profile Data*

A sub-bottom profiling system was used to acquire high-resolution sonar sub-bottom data. The system transmits an FM pulse that is linearly swept over a full spectrum frequency range, providing maximum penetration while maintaining high-resolution. The sub bottom profiler has a separate transmitter and separate acoustic receivers. Separated transmitting and receiving arrays are used to preserve linearity and to allow simultaneous transmission and reception. The acoustic return received is passed through a pulse compression filter, generating high-resolution images of the sub-bottom stratigraphy in offshore waters. The acquired data was logged digitally with position data output from Eiva Navipac in real-time to the subbottom profiler. During the period of surveys, sub-bottom penetration with the Edge Tech sub-bottom profiler system was aquired along the cross lines and the main lines within the area of investigation due to the presence of buried pipelines. During

the sub-bottom survey, several gain settings and transmitting frequencies were employed trying to resolve subsurface information. The signal penetration revealed depths to buried pipes.

*2.3.4 Magnetometer Data*

The MagPick Software package was used to process the mmagnetomete data. Internal functions available in MagPick shall be used to perform the Projection Transformation. MagPick allows the user to pick the magnetic anomalies either manually or automatically. All the magnetic anomalies of the survey area were picked manually as the Manual Target Picking option offers more flexibility. The magnetic anomaly map was generated to present the spatial disposition of the magnetic anomalies of the survey area.

***2.4 Data Interpretation***

*3.1 Bathymetry*

The power of amultibeamsystemlies in its ability to resolve sedimentary structures at wavelengths small enough to infer the processes active [4]. Many of the sediment transport mechanisms can be inferred from the short wavelength relief. Most notably, bedforms, such as transverse dunes or ripples and longitudinal ribbons provide a clear indication of active sediment transport. Similarly, erosional scour and pockmarks are indicative of modern or relict sedimentary processes. However, such features, which have spatial scales of decimetres to a few tens of metres, often lie at the limit of the spatial resolution of the system [5]. In the case of surface hull-mounted sonars, the resolution decays roughly linearly with depth. However, the question needs to be asked: does the disappearance of specific short wave length morphology with depth indicate a change in sedimentary environment, or merely a defocusing of the instrument over increasing range. Sedimentologists wishing to conduct multibeam surveys may not have the luxury of choice of system due to logistical or financial constraints. When interpreting the available data, however, it is important to establish the achievable resolution of the utilized specific sonar system [3].

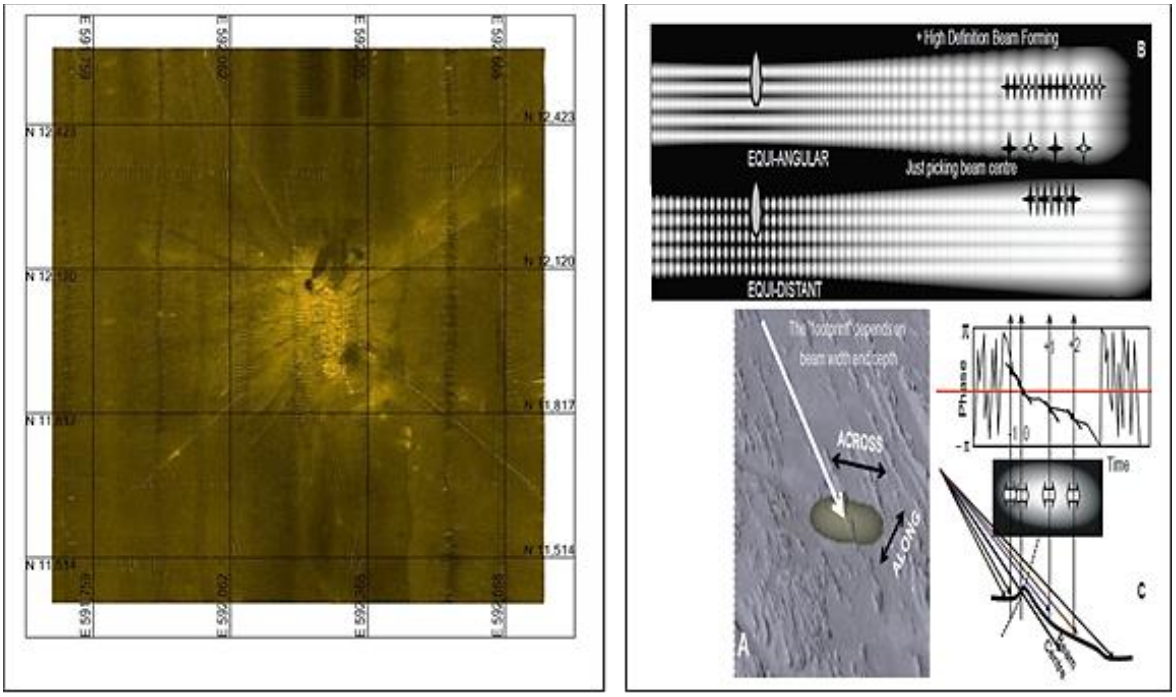


**Figure 4:** Representation of an oblique narrow beam footprint on a typical seabed terrain and Variation of size and spacingof a series of multibeam profiles.

Achievable resolution is no guarantee of absolute survey accuracy at that level. Any survey consists of a series of systematically offset corridors of data, normally called swaths. The combination of

multiple swaths requires a common reference datum. Absolute accuracy limits will corrupt the data in two ways: (1) when blending the overlap, the view of the seabed in the region of overlap will be defocused; and (2) when comparing the swath with data collected at other times, only scales of seabed change larger than the combination of the achievable accuracies of both surveys will be discernable. Sound speed [3], reducing the angular sector of the swath, and reviewing archived information about likely water mass variability and then designing the survey to take that into account.

*3.4.1 Backscatter*

Increasingly, spatial variations in the seabed backscatter strength are being used as an additional tool to aid in interpretation of shelf sedimentary processes. In order to use this effectively, a proper understanding of both the physical controls on seabed scattering and the effect of sonar radiometric and geometric imaging is required. Physical controls on seabed scattering Seabed backscatter strength is driven by the seabed's physical properties [11] and thus is potentially a useful indicator of sedimentary environment. A direct correlation between acoustic backscatter strength and a simple was used.

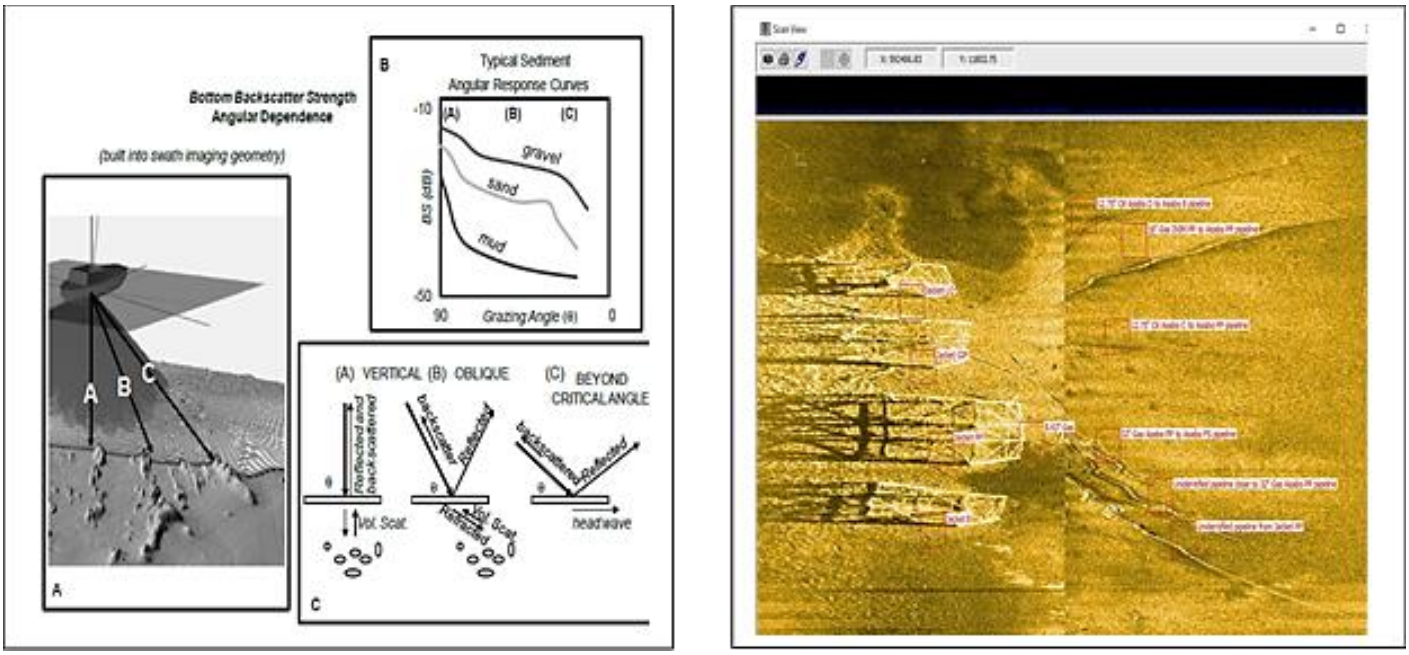


**Figure 5:** The effect of grazing angle on multibeam geometry and typical angular response curves.

Quantity such as grain size has been inferred [1] but in general remains elusive because spatial variations in backscatter may reflect changes in one or all of the following: Impedance contrast of the seabed/seawater interface (controlled by the bulk density and sound speed in the sediment); Interfacial roughness of that sediment water boundary; Volume heterogeneity – changes in the patchiness and contrast in the very shallow subsurface impedance; Changing grazing angle (Figure 2). Even at a fixed grazing angle, it can thus be ambiguous as to whether a change viewed is resulting from a change in impedance, roughness, or volume heterogeneity.[8] demonstrated that, for terrigenous sediments, the impedance is strongly correlated with grain size. It would be convenient if this were the principal control on backscatter strength but, for a given grain size, the interface roughness is linked to other factors such as sorting or rippling or the presence of shell hash. For fine-grained sediment (where there is significant penetration into the sediment), the volume heterogeneity is controlled strongly by bioturbation and/or the presence or absence of buried shell debris or glacial drop stones.2dB are still common and hamper interpretation of typical continental shelf seabed sediment signatures that are of similar magnitude[10]. Given all the imperfections outlined above, the real-time backscatter output of the multibeam sonar systems will contain artifacts that hamper the ability to undertake regional sediment distribution analysis. The most noticeable

effect is that of residual beam pattern and grazing angle distribution. Thus strategies need to be developed to minimize these artifacts. Estimating residual beam pattern and grazingangle variabilityIn order to remove the beam pattern and grazing angle effects, one ideally needs to know the transmit and receive beam pattern sensitivities (by sonar and/or vertically referenced angle, as well as the local seabed angular response curve (by seafloor grazing angle, Figure 2).

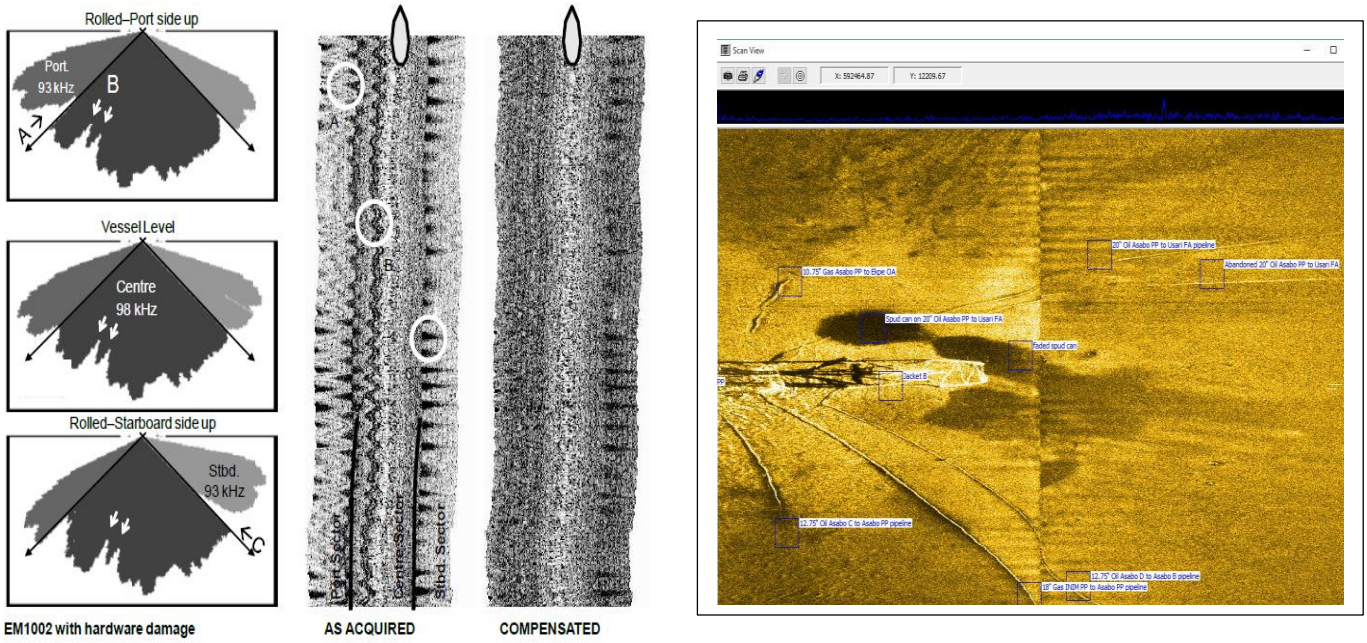


**Figure 6:** Special case processing for multi-sector multibeam backscatter data.

### 3. Results and Discussion

The research results consist of bathymetric and geophysical survey data and are presented in the following sections.

Water depth ranges between 41.88m to 45.46m within the Mfotu survey Corridor. The sonar records of the Mfotu infer the dominant presence of Low Reflective Sediments, interpreted to be composed of Silty Clayey SAND, all over the field Survey corridor. However, High reflective sediments, interpreted to be composed of Clayey, Silty SAND was observed as patches around, pipeline and the MfotuPlatform Area. The major seabed feature of the Mfotu Survey corridor is uniformsand waves regimes indicative of underwater current shaping the seabed of the survey corridor resulting in the accumulation of High Reflective Sediments observed around the detected pipelines and field Platform Area.

Existing and faded spud can foot prints of previous work rigs were observed on the sonar record of the Mfotu survey corridor.The sides scan sonar data of the 500m radius surveyed area around the Mfotu B and LQ jackets was consistent with the survey chart provided by MPN. The data showed high reflective discrete returns on subsea installations like the Mfotu B, PP and LQ Jackets. It also, showed two unidentified pipelines and all the pipelines entering the jackets except for the 4.5'' Gas Mfotu A to Mfotu PP pipeline which is buried. One of the unidentified pipeline is running South East from Jacket GIP and the other looks abandoned as one end lies close to Jacket PP and the other end appeared ruptured as a piece of conductor about 370m also South East of Mfotu PP. Debris measuring about 9.5m and about 350m North East of Jacket B was also seen and Spud can be observed on the 20'' Oil Mfotu PP to Mfotu FA pipeline also close to Mfotu B Jacket.

**Table 2:** Mfotu Side Scan Sonar Processed Data

| Mfotu SSS Processed Data | | | | | | |
|---|---|---|---|---|---|---|
| **Feature** | **code** | **Easting** | **Northing** | **Length (m)** | **Width (m)** | **orientation (°)** |
| **Jacket** | Jacket1 | 592268.09 | 12082.12 | 25 | 18 | 360 |
| | Jacket 2 | 592269.43 | 12028.7 | 37 | 24 | 360 |
| | Jacket 3 | 592283.61 | 11963.29 | 49 | 25 | 357 |
| | Jacket 4 | 592290.15 | 11904.81 | 24 | 24 | 357 |
| **Debris** | Deb | 592021.17 | 12322.32 | 9.5 | NIL | 284 |
| **Spud can** | sp | 592238.65 | 12081.99 | | | |
| **Faded spud can** | Fsp1 | 592252.63 | 12109.96 | | | |
| **Faded spud can** | Fsp2 | 592297.54 | 12103.51 | | | |
| **12.75" Oil Pipeline** | Point 1 | 592305.62 | 12074.63 | | | |
| | Point 2 | 592327.64 | 12087.97 | | | |
| | Point 3 | 592349.86 | 12102.51 | | | |
| | Point 4 | 592379.36 | 12122.31 | | | |
| | Point 5 | 592396.01 | 12133.89 | | | |

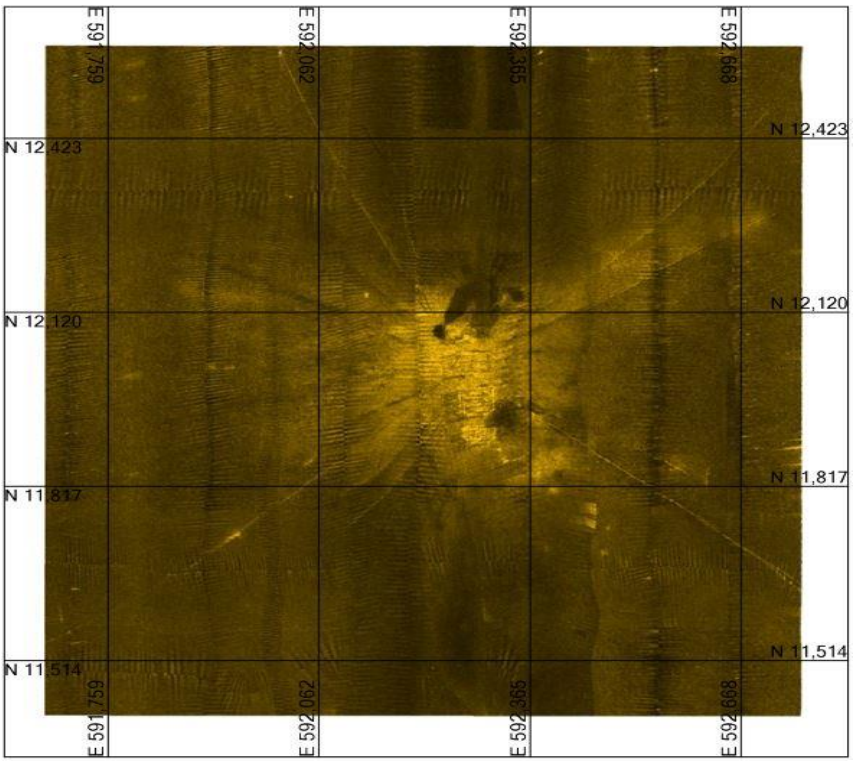


**Figure 7:** Mfotu 500m Radius Mossaic

All captured pipelines are entirely exposed except the 4.5″ gas Mfotu A to Mfotu PP within the survey corridor. Sand waves are the major seabed features characterizing the field Platform Area causing sediment accumulations around pipeline and platform structures. No spudcan depressions were observed on the sonar records of the study area. Besides the pipelines, debris with length 9.5m and 350m north east of Jacket B was detected. A piece of conductor about 370m south east of Mfotu PP was also observed on the sonar record.

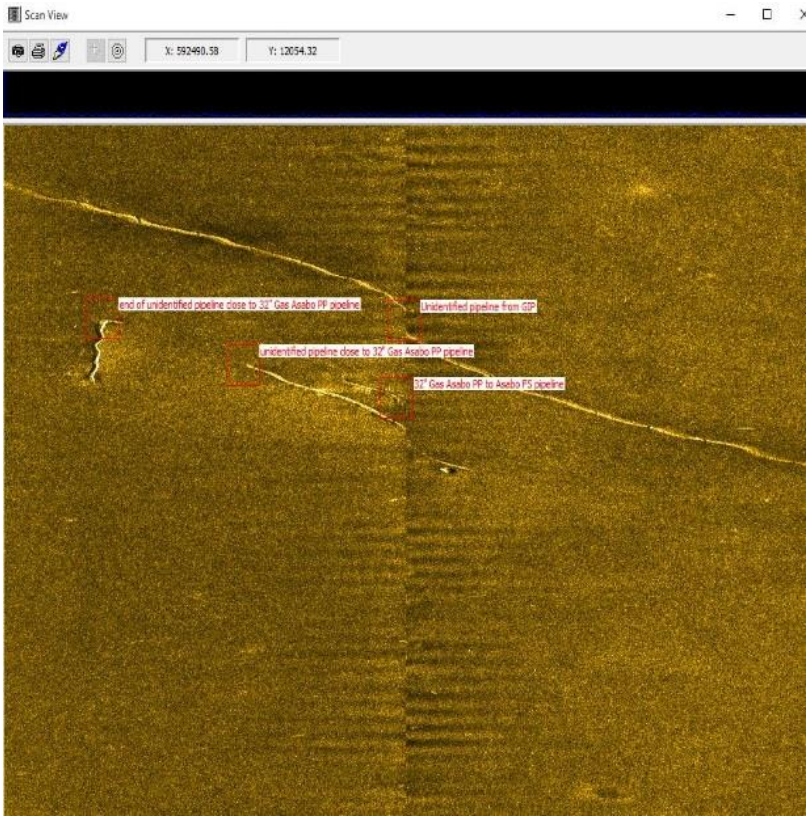


**Figure 8:** Screen shot showing 350m radius Mfotu B and LQ Jacket

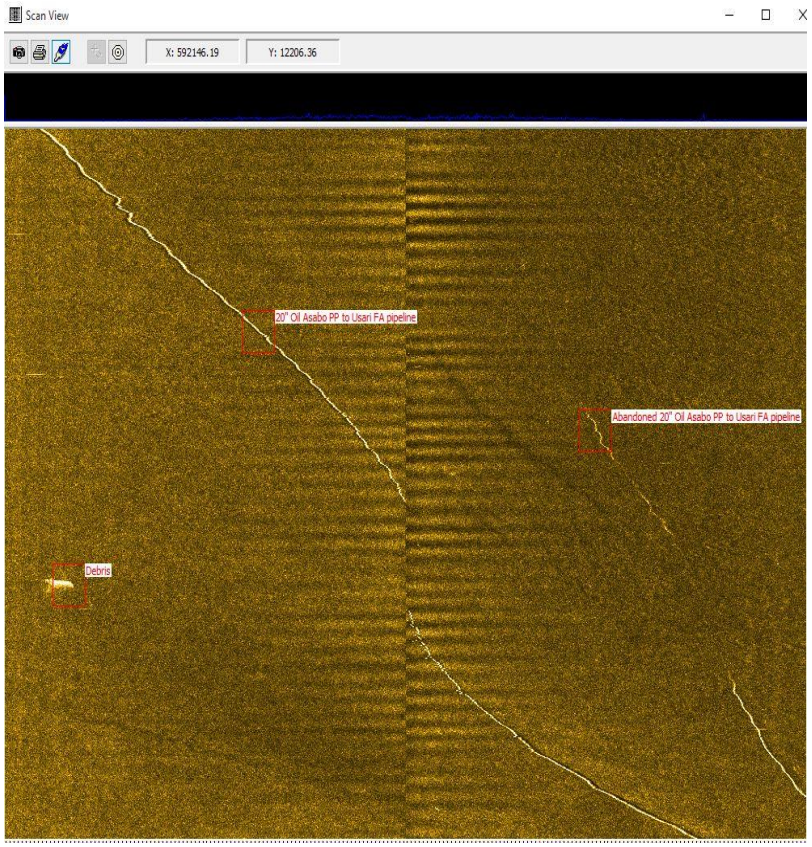


**Figure 9:** Screen Shot Showing 250m Radius of Mfotu B and LQ Jacket

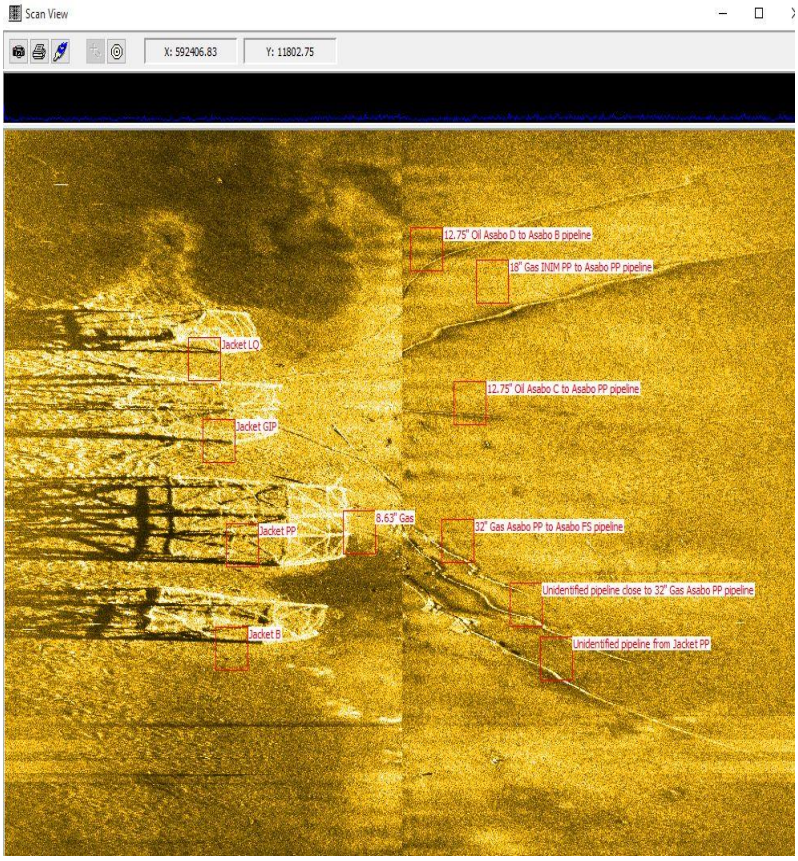


**Figure 10:** Screen Shot showing Mfotu B, PP, GIP, LQ Jackets, 12.75'' Oil Mfotu D to Mfotu B, 18'' Gas INIM PP to Mfotu PP, 12.75'' Oil Mfotu C to Mfotu PP, 8.63'' Gas Mfotu GIP to Mfotu C , 32'' Gas Mfotu PP to Mfotu FS, Unidentified pipeline close to 32'' Gas Mfotu PP and Unidentified pipelines.

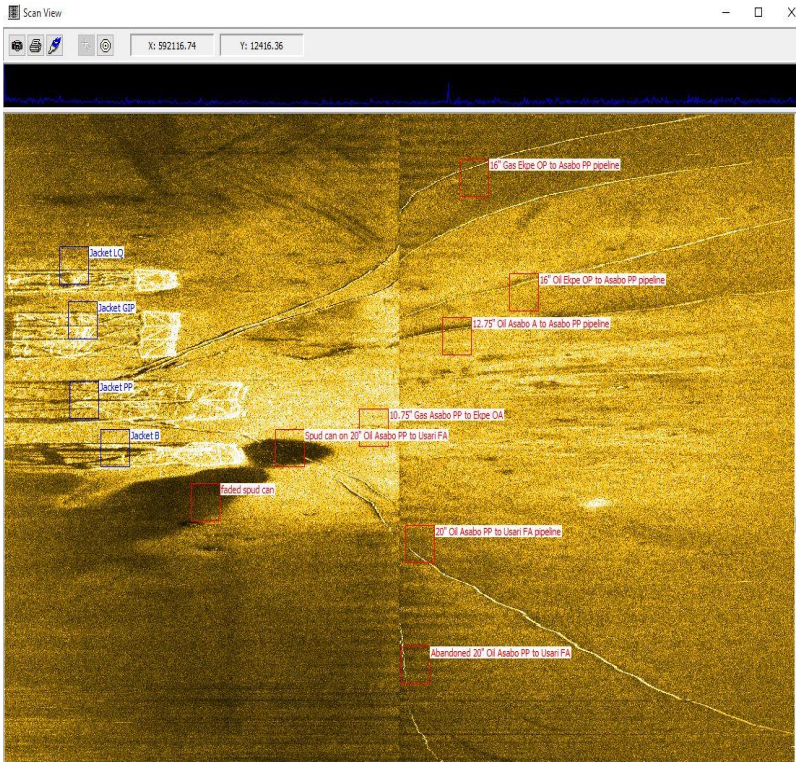


**Figure 11:** Screen Shot showing Mfotu B, PP, GIP, LQ Jackets, 16'' Gas Mfotu OP to Mfotu PP, 16'' Oil Ekpe OP to Mfotu PP, 16'' Oil Mfotu OP to Mfotu PP, 12.75'' Oil Mfotu A to Mfotu PP, 20'' Oil Mfotu PP to abandoned 20'' Oil Mfotu PP to FA pipelines and spud cans

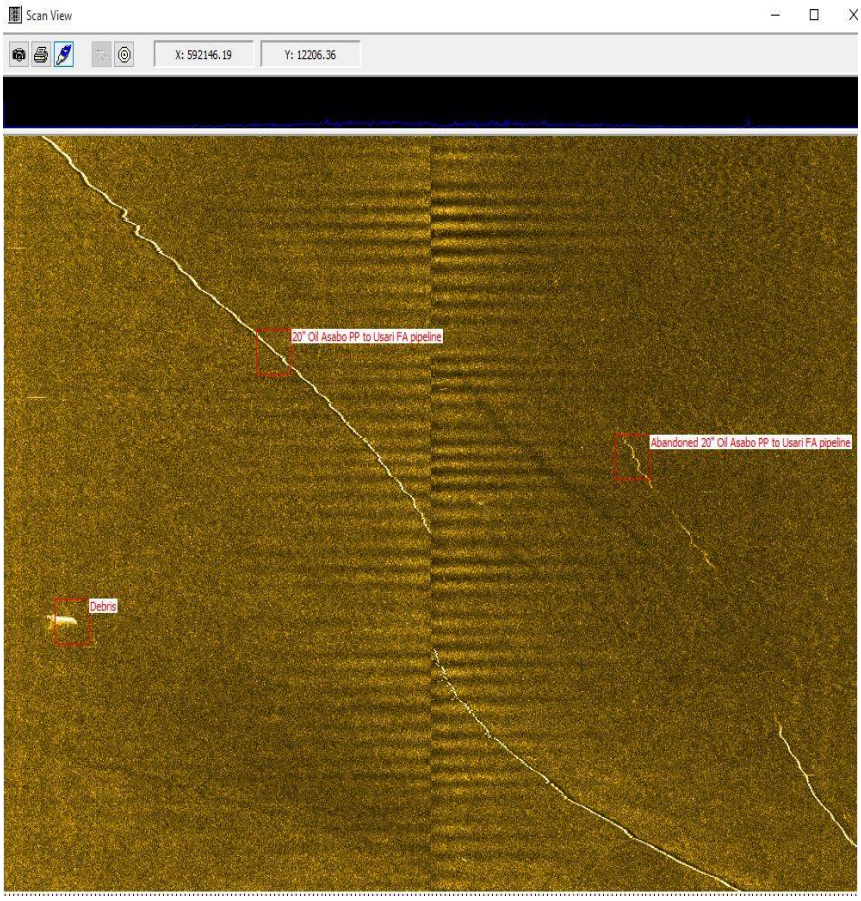


**Figure 12:** Screen Shot showing Abandoned 20'' Oil Mfotu PP to FA, 20'' Oil Mfotu PP to FA pipelines and Debris

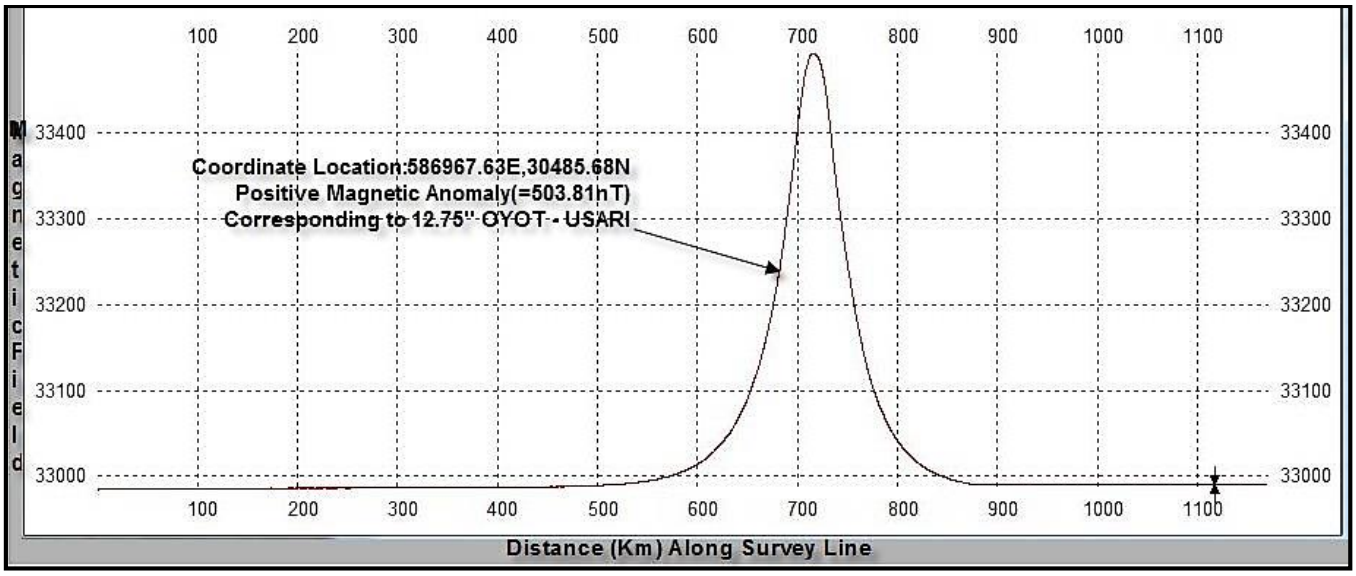


**Figure 13:** Maggy Data Extract Showing Exposed Pipeline detected at Mfotu Platform Area

Magnetic anomalies observed within the Mfotu MP surveyed corridor were due to existing pipelines and platform structures. Details are provided in figure 10, and table 2. The Sub bottom Profiler data for MfotuArea showed the seabed location between 23ms to 24ms and the seabed multiple coming at approximately 48ms. The data is limited to no more than 15ms (12m, ASV 1600m/s) of interpretable data due to limited penetration and random burst of noise within the data. More regular noise has been removed with a frequency filter. The subbottom profiler data is uniform

across the survey area showing one reflector the varies between 1.22m and 1.52m below seabed.The detected 12.75'' OIL pipeline Mfotu to FA was found to be exposed on the seabed. Please refer to figure 6 next page for details. No other significant structure can be seen within the data set underlying the reflector underneath the seabed apart from the tails of diffractions from various pipelines within the Mfotu A survey corridor.

Table 3: Positions of the Magnetic Anomalies

| Magnetic | Position of the Anomaly | | Amplitude (nT) | Type |
|---|---|---|---|---|
| Contact ID | Easting (m) | Northing (m) | | |
| ASA1 | 591889.791 | 11600.516 | 1.22nT | Positive Anomaly |
| ASA2 | 591890.302 | 11687.839 | 77.74nT | Negative Anomaly |
| ASA3 | 591889.905 | 11704.013 | 115.00nT | Dipole |
| ASA4 | 591908.097 | 11837.609 | 177.34nT | Dipole |
| ASA5 | 591913.721 | 12020.322 | 313.40nT | Negative Anomaly |
| ASA6 | 591895.918 | 12162.981 | 503.81nT | Positive Anomaly |
| ASA7 | 591987.401 | 12630.795 | 121.32nT | Negative Anomaly |
| ASA8 | 592035.838 | 12305.921 | 44.96nT | Negative Anomaly |
| ASA9 | 592018.521 | 12131.918 | 16.84nT | Positive Anomaly |
| ASA10 | 592026.492 | 12018.52 | 21.55nT | Negative Anomaly |
| ASA11 | 591996.671 | 11841.908 | 43.43nT | Positive Anomaly |

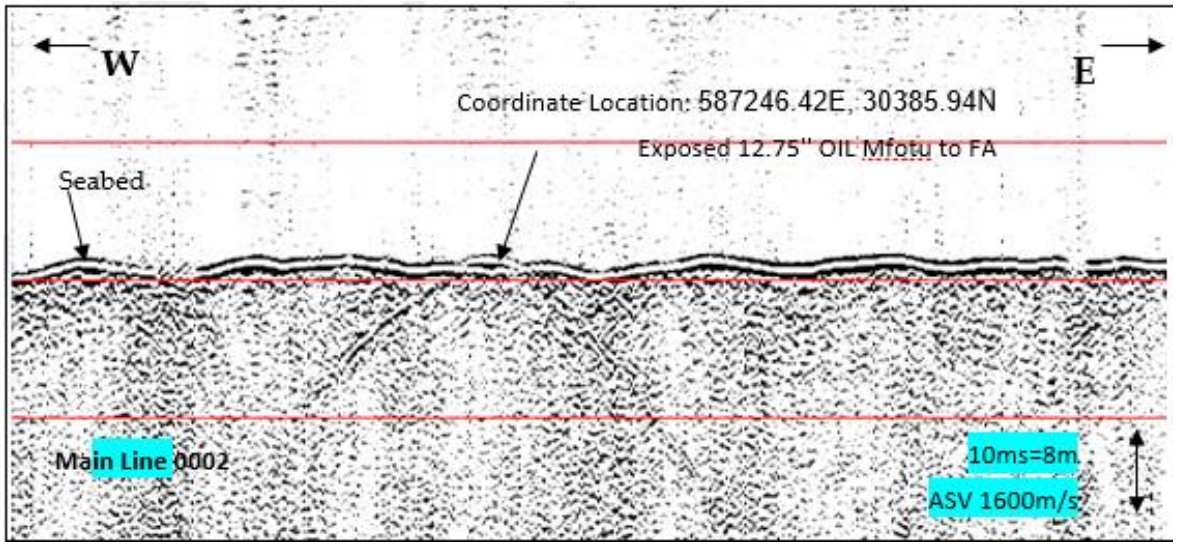


**Figure 14:** SBP Data Extract of Survey Main Line Showing Exposed Pipeline Southeast of Mfotu A.

## 4. Conclusions

Multibeam bathymetry and backscatter are providing an unprecedented view of co-located bottom morphology and surficial sediment distribution over continental shelf areas. The following survey information concludes the seabed survey of Mfotu MP carried out October 9th and November 4th 2018.The water depth ranges between ranges between 41.88m to 45.46m within the Mfotu MP surveyed corridor.The sonar records of the MFOTU MP infer the dominant presence of Low Reflective Sediments, interpreted to be composed of Silty Clayey Sand, all over the Mfotu MP survey corridor.The magnetic anomalies observed within the field survey corridor were due to existing pipeline and platform structures.The seismic profile of the Mfotuarea suggests variation in sediment thickness between 1.22m and 1.52m.No other significant structure can be seen within the data set underlying the reflector underneath the seabed apart from the tails of diffractions from the existing Pipelines running in and out of Mfotu, conductor and debris. All existing pipelines are completely exposed except the 4.5’ gas Mfotu A to MfotuPP pipeline within the survey corridor. There are existing faded spudcans observed and foot prints of previous work rigs at Mfotu MP. However, sand

waves are the major seabed features characterizing the Mfotu MP Survey corridor. Two unidentified pipelines were detected entering the jackets. One of the unidentified pipeline is running South East from Jacket GIP and the other looks abandoned as one end lies close to Jacket PP and the other end appeared ruptured as a piece of conductor about 370m also South East of Mfotu PP. Debris measuring about 9.5m and about 350m North East of Jacket B was also seen. It should be noted that the detected two 32' gas pipelines closed to Mfotu MP and unidentified pipeline from GIP Jacket are not on the MPN drawing provided for Mfotu MP Seabed Location. It is thus recommended that charts be updated with these latest findings to reflect the current survey outcome detailing the seabed conditions and facilities at Mfotu MP. From the observed sonar record of the Mfotu MP survey corridor, there is no significant seabed features or obstructions that may pose constraints or hazards to the planned JUB move.

**5. Recommendations**

Rig to proceed with the planned Movement and operations considering the critical survey information presented above.The topography of the Mfotu field seafloor should be investigated periodically for the integrity of subsea facilities. Trenching should be carried out during the emplacement of pipelines in the Northern part of the field due to turbulence.

**Funding:** Not applicable.

**Institutional Review Board Statement:** Not applicable.

**Informed Consent Statement:** Not applicable.

**Acknowledgments:** Not applicable**.**

**Conflicts of Interest:** The authors declare no conflict of interest.

## References

1. Borgeld, J.C., Hughes Clarke, J.E., Goff, J.A., Mayer, L.A.and Curtis, J.A. **(1999)**. Acoustic backscatter of the 1995 flood deposit on the Eel shelf. *Mar. Geol.* 154: 197–210.
2. Brucker, S., Hughes Clarke, J.E., Beaudoin, J., Lessels, C., Czotter, K., Loschiavo, R., Iwanowska, K. and Hill, P. **(2007)**. Monitoring flood-related change in bathymetry and sediment distribution over the Squamish Delta, Howe Sound, British Columbia. *US Hydrogr. Conf. 2007*, CDROM, 16 pp.
3. Cartwright, D. and Hughes Clarke, J.E. **(2002)**. Multibeam surveys of the Frazer River Delta, coping with an extreme refraction environment. *Can. Hydrogr. Conf. Proc.* CDROM., 22 pp.
4. Chuku, H.C. and Ibe, A.C. **(2015)**. Topography and Lithofacies of the seafloor in Meren field, *offshore Western Niger Delta. IJSIT*, 4(6):524-551.
5. Chuku, C.H., Odigi, M.I., Ibe, C.A. and Ideozu, R.U. **(2018)**. Geophysical and geotechnical investigations of the seafloor sediments for offshore subsea facility installation in "Emobs" oil fields, Western Niger Delta Nigeria. *AJARR.40989*, 1(1):1-16.
6. Duffy, G.P. and Hughes Clarke, J.E. **(2005).** Application of spatial cross-correlation to detection of migration of submarine sand dunes, Special Publication on Marine and River dune dynamics, *J.Geophys. Res*., 110, F04S12.
7. Gardner, J.V., Dartnell, P., Mayer, L.A., Hughes Clarke, J.E., Calder, B.R. and Duffy, G. **(2005).** Shelf-edge delta and drowned barrier island complexes on the Northwest Florida outer continental shelf. *Geomorphology* 64, 133–166.
8. Hamilton, E.L. and Bachman, R.T. **(1982).** Sound velocity and related properties of marine sediments. *J. Acoust. Soc. Amer*. 72, 1891–1904.
9. Hughes Clarke, J.E., Mayer, L.A. and Wells, D.E. **(1996).** Shallow-water imaging multibeam sonars: Anewtool for investigating seafloor processes in the coastal zone and on the continental shelf. *Mar. Geophys. Res.* 18, 607–629.
10. Iwanowska, K., Hughes Clarke, J.E., Conway, K.W. and Barrie, V. **(2005).** Managing systematic residual errors in multibeam backscatter data. GEOHAB 2005, Victoria, *Conf. Prog.with abstracts,* 80–81.
11. Jackson, D.R., Winebrenner, D.P. and Ishimaru, A. **(1986).** Application of the composite roughness model to high frequency bottom backscattering. *J. Acoust. Soc.Am*. 79, 1410–1422.
12. Kammerer, E., Hughes Clarke, J.E., Locat, J., Doucet, N. and Godin, A. **(1998).** Monitoring temporal changes in seabed morphology and composition using multibeam sonars: a case study of the 1996 Saguenay River floods. *Proc. Can. Hydrogr. Conf.* 1998, Victoria, 450–461.
13. Sonnichsen, G.V., King, T., Jordan, I. and Li, C. **(2005).** Probabilistic analysis of iceberg scouring frequency based on repetitive seabed mapping, offshore Newfoundland and Labrador. *Proc. 18th Int. Conf. Port Ocean Eng. under Arctic.*

*Cite article as:*

Chuku, H. C., Umoh, E.E., Agbaje, P.O. Seafloor Sediments Morphodynamics: Implications on Subsea Facilities in Mfotu field offshore Eastern Niger Delta Nigeria. *Ajayi Crowther J. Pure Appl. Sci.* **2023**, 2(1): 47-59. https://doi.org/10.56534/acjpas.2023.02.01.47.